the carbonyl would interrupt this interaction.

As a very simple example, let us consider two metals each with an orbital appropriate for π bonding and a single carbonyl group with a π acceptor orbital. We will represent the π orbital on each metal by only one lobe, **4**, and the carbonyl π acceptor orbital by a p orbital on carbon, **5**. In a saturated M–M system both

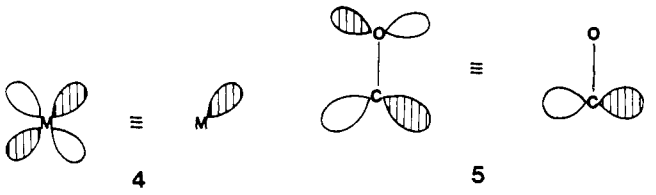

4 **5**

6 **7**

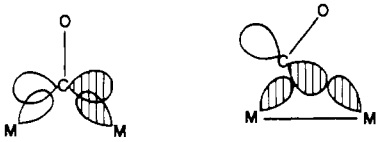

8 **9**

the symmetric combination of metal π orbitals, **6**, and the antisymmetric combination, **7**, are occupied. A carbonyl group will achieve maximum interaction with this system by orienting itself perpendicular to the M–M bond axis so that its π acceptor orbital interacts with the antisymmetric combination, **7**. The resulting occupied orbitals will then be **6** and **8**. In an unsaturated M–M system only the symmetric combination, **5**, will be occupied. In order to stabilize this system the carbonyl group will turn to present only one lobe of the π acceptor orbital to the metals, forming a three-center, two-electron bond. In this case only the 3-c, 2-e bond, **9**, is occupied. Our results also explain the nature of the bonding found in metal carbonyl fragments bonding to Lewis acids.[18] Here, the linear semibridging CO is interacting with the occupied dative (d_π metal $\rightarrow$ p_π acid) MO, while the corresponding antibonding combination is empty. Recently, Bênard, Dedieu, and Nakamura have suggested a similar model to explain the linear, semibridging carbonyl in $Mn_2(CO)_5(dppm)_2$.[19]

The calculations do not completely explain why the M–M–Cp angle is linear when M = Mo but bent 15° when M = Cr. For a fixed $M_2(CO)_4$ (M = Cr, Mo) fragment, contacts between the ring and the carbonyls are decreased as the cyclopentadiene ring is bent. The larger molybdenum atoms allow this distance to increase so that steric crowding does not influence the bonding and structure in the molybdenum species. The 15° Cr–Cr–Cp bend is a minor structural change in order to accomodate these nonbonding repulsions. Although this may not be the only reason for the bend, it is the only one offered by our calculations.

With the above explanation in mind, the ionizations at 7.25 and 8.80 eV in the spectrum of the chromium species can be readily explained. These bands were assigned as ionizations from the $15b_u$ and $14a_g$ orbitals, respectively. As the distortion to a nonlinear M–M–Cr angle occurs the $14a_g$ orbital becomes less stable, and its ionization now appears before the Cp ionizations. The $11a_u$ and $14b_u$ orbitals are stabilized, which isolates the $15b_u$ orbital and it appears well separated from the other M ionizations. These results support the idea that the series $[CpM(CO)_2]_2$ would prefer a linear M–M–Cp angle and that as this angle is decreased the $15b_u$ and $14a_g$ orbitals reflect this relative destabilization and move to lower IE.

Acknowledgment. We gratefully acknowledge the support of the Robert A. Welch Foundation (Grant No. A-648) and the National Science Foundation (Grant No. CHE79-20993 and CHE83-09936) as well as the gift of the compounds from Professor M. David Curtis (University of Michigan).

(18) Curtis, M. D.; Han, K. R.; Butler, W. M. *Inorg. Chem.* **1980**, *19*, 2096 and references therein.
(19) Bênard, M.; Dedieu, A.; Nakamura, S. *Nouv. J. Chim.* **1984**, *8*, 149.

Electron-Transfer Fluorescence Quenching of Radical Ions. Experimental Work and Theoretical Calculations

Jens Eriksen,* Karl Anker Jørgensen,* Jan Linderberg, and Henning Lund

Contribution from the Department of Chemistry, University of Aarhus, DK-8000 Aarhus C, Denmark. *Received December 29, 1983*

Abstract: The fluorescence of the anthraquinone radical anion and the thianthrene radical cation is quenched via an electron-transfer mechanism by added electron acceptors and donors, respectively. The quenching data are treated in terms of the Marcus theory leading to very large reorganization energies, ΔG^*_0 (10.0 and 15.3 kcal/mol for the two radical ions). Apparently the Weller equation is less suited for treatment of the fluorescence data in these systems. The large reorganization energies are analyzed by theoretical calculations based mainly on the energy weighted maximum overlap (EWMO) model. According to these calculations the photochemically excited anthraquinone radical anion is folded into a geometry quite different from the planar ground state of anthraquinone thus resulting in a prediction of a large bond reorganization energy.

Electron-transfer fluorescence quenching continues as an active field of study among photochemists and photophysicists.[1-4] Most work in this field has been centered around electron transfer to or from the singlet excited state of fluorescing aromatic molecules

(1) Rehm, D.; Weller A. *Isr. J. Chem.* **1970**, *8*, 259.
(2) (a) Eriksen, J.; Foote, C. S. *J. Am. Chem. Soc.* **1980**, *102*, 6083. (b) Eriksen, J.; Plith, P. E. *Tetrahedron Lett.* **1982** *23*, 481.
(3) Maroulis, A. J.; Shigemitsu, Y.; Arnold, D. R. *J. Am. Chem. Soc.* **1978** *100*, 535 and references cited therein. Brown-Wensley, K. A.; Mattes, S. L.; Farid, S. *J. Am. Chem. Soc.* **1978**, *100*, 4162.

0002-7863/84/1506-5083$01.50/0

Table I. Fluorescence Data of Radical Ions[a]

fluorescer	solvent	emission max, nm	$\Delta E_{0,0}$,[b] eV	τ,[c] ns
$Aq^{-}\cdot$	DMF[d]	575	2.21	13.7
$Ta^{+}\cdot$	CH_2Cl_2[e]	580	2.18	4.7

[a] In fluid solution at room temperature. [b] Excitation energy. [c] Fluorescence lifetime. [d] Dimethylformamide. [e] Solvent mixture of methylene chloride, trifluoroacetic anhydride, and trifluoroacetic acid (45:5:1 v/v).

in the presence of electron donors (D) or acceptors (A), respectively. The reaction is thus accompanied by fluorescence quenching of the light-absorbing molecule:

$$\begin{matrix} A \xrightarrow{h\nu} {}^1A^* \\ D \xrightarrow{h\nu} {}^1D^* \end{matrix} \begin{matrix} \xrightarrow{D} \\ \xrightarrow{A} \end{matrix} [D^{\delta+}\cdots A^{\delta-}] \rightleftharpoons D^{+} + A^{-}$$

We have for some time been interested in electron transfer from photoexcited radical ions, which were produced electrochemically.[5,6] It was shown[6] that a plot of the rate constants of the

$$D \xrightarrow{e} D^{-}\cdot \xrightarrow{h\nu} (D^{-}\cdot)^* \xrightarrow{A} [D\cdots A]^{-}\cdot \rightarrow D + A^{-}\cdot$$

$$A \xrightarrow{-e} A^{+}\cdot \xrightarrow{h\nu} (A^{+}\cdot)^* \xrightarrow{D} [A\cdots D]^{+}\cdot \rightarrow A + D^{+}\cdot$$

electron transfer vs. the free energy of the reaction could fit neither the Marcus equation nor the Weller equation when the usual assumption of the magnitude of the reorganization energies of such reactions was made. The radical ions studied included the anthraquinone radical anion ($Aq^{-}\cdot$) and the thianthrene radical cation ($Ta^{+}\cdot$).[6]

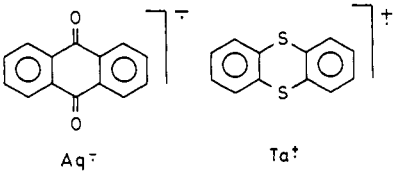

Aq^{-} Ta^{+}

We now wish to report that the fluorescence quenching can be interpreted in terms of the Marcus theory with very large activation barriers. Thus, our results confirm the predictions and recent results by Eberson,[7,8] who has argued that the widely accepted activation barrier of 2.4 kcal/mol need not and indeed should not be valid for all electron-transfer reactions. We also find that these large energy barriers for our systems may be understood on the basis of (large) geometric changes in the electron-transfer process as revealed by theoretical calculations.

Results and Discussion

As previously reported[6] the radical ions $Aq^{-}\cdot$ and $Ta^{+}\cdot$ fluoresce in oxygen-free solutions at room temperature. The fluorescence data are summarized in Table I.

The fluorescence of $Aq^{-}\cdot$ and $Ta^{+}\cdot$ was quenched by added electron acceptors and donors, respectively. In each case, the quenching followed the well-known Stern–Volmer equation[9]

$$I_0/I_Q = 1 + k_q\tau[Q] \qquad (1)$$

Table II. Fluorescence Quenching of $Aq^{-}\cdot$[a]

quencher	$10^{-9}k_q$,[b] M^{-1} s^{-1}	$E^\circ_{A/A^{-}\cdot}$,[c] V vs. SCE	ΔG,[d] kcal/mol
acridine	13.9	−1.63[e]	−33.4
benzophenone	12.0	−1.77[e]	−30.2
1-naphthonitrile	11.0	−1.90[e]	−27.2
2-chloroquinoline	13.6	−1.92[f]	−26.8
3-cyanopyridine	4.89	−2.03[e]	−24.2
1-bromonaphthalene	2.70	−2.13[f]	−21.9
1-chloronaphthalene	1.61	−2.19[f]	−20.5
benzonitrile	0.708	−2.23[e]	−18.2
3-bromopyridine	0.562	−2.29[f]	−17.3
3-chloropyridine	0.095	−2.39[f]	−15.9
2-chloropyridine	0.102	−2.40[f]	−15.7
bromobenzene	0.036	−2.44[f]	−14.8

[a] In oxygen-free DMF at room temperature. [b] Slope of Stern–Volmer plot (eq 1) divided by lifetime (Table I). [c] Reduction potential. [d] Calculated from eq 2, $E^\circ_{Aq/Aq^{-}\cdot} = -0.87$ V vs. SCE (ref 6). [e] Determined by reversible cyclic voltammetry (ref 6). [f] Determined by kinetic analysis of homogeneous redox catalyses of electronic reductions. Data from: Andrieux, C. P.; Blocman, C.; Dumas-Bouchiat, J.-M.; and Savéant, J. M. *J. Am. Chem. Soc.* **1979**, *101*, 3431. Andrieux, C. P.; Blocman, C.; Dumas-Bouchiat, J. M.; M'Halla, F.; Savéant, J. M. *Ibid.* **1980**, *102*, 3806.

Table III. Fluorescence Quenching of $Ta^{+}\cdot$[a]

quencher	$10^{-9}k_q$,[b] M^{-1} s^{-1}	$E^\circ_{D^{+}\cdot/D}$,[c] V vs. SCE	ΔG,[d] kcal/mol
pyrene	7.23	1.36[e]	−46.8
acenaphthene	6.11	1.52[f]	−43.1
hexamethylbenzene	5.32	1.61[e]	−41.0
anisole	1.38	1.76[f]	−37.6
naphthalene	0.957	1.84[e]	−35.7
thiophene	0.140	2.03[f]	−31.4

[a] In oxygen-free CH_2Cl_2/trifluoroacetic anhydride/trifluoroacetic acid (45:5:1) at room temperature. [b] Slope of Stern–Volver plot (eq 1) divided by lifetime (Table I). [c] Polarographic half-wave oxidation potential. [d] Calculated from eq 3, $E^\circ_{Ta^{+}\cdot/Ta} = 1.21$ V vs. SCE (ref 6). [e] Data from Table IX in: Eberson, L. *Adv. Phys. Org. Chem.* **1982**, *18*, 79. [f] Data from: Eberson L., private communication.

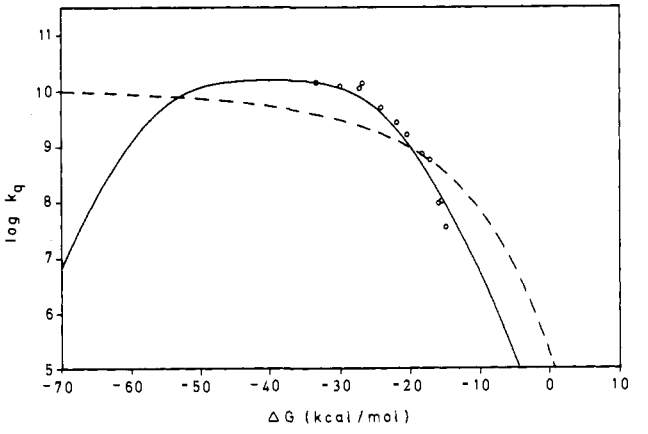

Figure 1. Weller plot for $Aq^{-}\cdot$ of k_q (from eq 1) vs. ΔG (from eq 2): (—) optimized curve based upon the Marcus equation (eq 4 and 6) with $\Delta G^{\ddagger}_0 = 10.0$ kcal/mol; (- - -) optimized curve based upon the Weller equation (eq 4 and 5) with $\Delta G^{\ddagger}_0 = 7.6$ kcal/mol. Experimental data from Table II.

where I_0 and I_q are the relative fluorescence intensities in the absence and presence of quencher (Q), respectively, k_q is the bimolecular quenching rate constant, and τ is the fluorescence lifetime. From plots of I_0/I_Q vs. [Q] and τ (Table I) k_q could be extracted; see Tables II and III.

The free energy change (ΔG) involved in an electron-transfer process from an excited donor radical anion to a neutral acceptor is given by eq 2,[1,6] where $E_{D/D^{-}\cdot}$ is the reversible electrode potential

$$\Delta G \text{ (eV)} = E^\circ_{D/D^{-}\cdot} - E^\circ_{A/A^{-}\cdot} - \Delta E_{0,0} \qquad (2)$$

of the fluorescer couple $D/D^{-}\cdot$, $E_{A/A^{-}\cdot}$ is that of the acceptor couple,

(4) (a) Iwa, P.; Stelner, U. E.; Vogelmann, E.; Kramer, H. E. A. *J. Phys. Chem.* **1982**, *86*, 1277. (b) Kawenoki, I.; Keita, B.; Kossanyi, J.; Nadjo, L. *Nouv. J. Chem.* **1982**, *6*, 387. (c) Eriksen, J.; Foote, C. S. *J. Phys. Chem.* **1978**, *82*, 2659. (d) Taylor, G. N. *Chem. Phys. Lett.* **1971**, *10*, 355. (e) Ware, W. R.; Watt, D.; Holmes, J. D. *J. Am. Chem. Soc.* **1974**, *96*, 7853. (f) Caldwell, R. A.; Ghali, N. I.; Chien, C.-K.; DeMarco, D.; Smith, L. *Ibid.* **1978**, *100*, 2857. (g) Lewis, F. D.; Ho, T.-I. *Ibid.* **1977**, *99*, 7991. (h) Yang, N. C.; Shold, D. M.; McVey, J. K. *Ibid.* **1975**, *97*, 5004. (i) Schaap, A. P.; Zaklika, K. A.; Kaskar, B.; Fung, L. W.-M *Ibid.* **1980**, *102*, 389. (j) Spada, L. T.; Foote, C. S. *Ibid.* **1980**, *102*, 391.

(5) Lund, H.; Carlsson, H. S. *Acta* Chem. *Scand., Ser. B* **1978**, *B32*, 505; **1980**, *B34*, 409.

(6) Eriksen, J.; Lund, H.; Nyvad, A. I. *Acta* Chem. *Scand., Ser. B* **1983** *B37*, 359.

(7) For a review, see: Eberson, L. *Adv. Phys. Org. Chem.* **1982**, *18*, 79–185.

(8) (a) Eberson, L. *Chem. Scr.* **1982**, *20*, 29. (b) *Acta Chem. Scand., Ser. B* **1982**, *B36*, 533.

(9) Turro, N. J. "Modern Molecular Photochemistry"; W. A. Benjamin: Menlo Park, 1978; p 247.

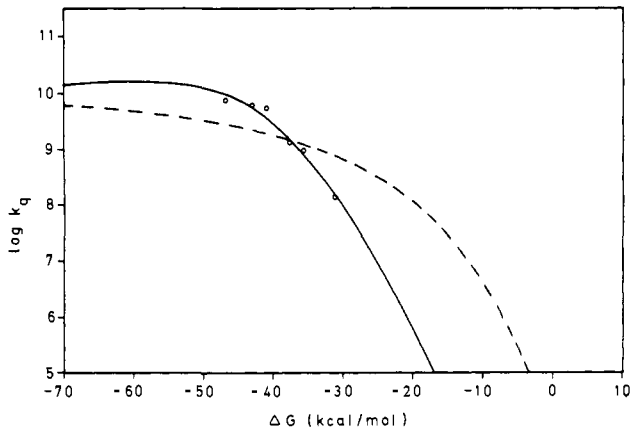

Figure 2. Weller plot for $Ta^{+}\cdot$ of k_q (eq 1) vs. ΔG (from eq 2): (—) optimized curve based upon the Marcus equation (eq 4 and 6) with $\Delta G^{\ddagger}_0$ = 15.3 kcal/mol; (---) optimized curve based upon the Weller equation (eq 4 and 5) with $\Delta G^{\ddagger}_0$ = 9.6 kcal/mol. Experimental data from Table III.

and $\Delta E_{0,0}$ is the excitation energy (Table I). Similarly, ΔG for quenching of an excited acceptor radical cation by neutral donors is given by eq 3.[6] Calculated ΔG values for $Aq^{-}\cdot$ (eq 2) and $Ta^{+}\cdot$

$$\Delta G\ (\text{eV}) = -E_{A^{+}\cdot/A} + E_{D^{*}\cdot/D} - \Delta E_{0,0} \qquad (3)$$

(eq 3) are listed in Tables II and III, respectively. Plots of k_q vs. ΔG (Weller plots[1]) are shown in Figures 1 and 2.

As the curves in Figures 1 and 2 differed from those in the usual Weller plot it was deemed necessary to ensure that the photochemically excited species was indeed $Aq^{-}\cdot$. Thus, it was necessary to test for possible protonation of $Aq^{-}\cdot$ by adventitious water in the DMF solution. Addition of 2 μL of water or a 1 M KOH solution to 2 mL of 10^{-5} M $Aq^{-}\cdot$ resulted in about a 10% decrease in the fluorescence intensity. Alternatively, addition of 2 μL of 1 M HCl or 1 M *p*-toluenesulfonic acid eliminates the emission immediately and completely. Further addition of excess base to the acidified solution did not revive the emission. Presumably, the protonated form of $Aq^{-}\cdot$ disproportionates irreversibly:

$$2Aq^{-}\cdot + 2H^{+} \rightarrow Aq + AqH_2$$

where AqH_2 represents 9,10-dihydroxyanthracene. Thus, it appears that the electrochemically produced $Aq^{-}\cdot$ indeed exists in this form in the DMF solution.

Rehm and Weller[1] have derived an empirical equation for the electron transfer fluorescence quenching rate constant, k_q:

$$k_q = \frac{2 \times 10^{10}\ M^{-1}\ s^{-1}}{1 \times 0.25[\exp(\Delta G^{\ddagger}/RT) + \exp(\Delta G/RT)]} \qquad (4)$$

where ΔG is given by eq 2 or 3 and $\Delta G^{\ddagger}$, the activation free enthalpy, is assumd to be a monotonic function of ΔG,

$$\Delta G^{\ddagger} = [(\Delta G/2)^2 + (\Delta G^{\ddagger}_0)^2]^{1/2} + \Delta G/2 \qquad (5)$$

Here, $\Delta G^{\ddagger}_0$, the activation free energy at $\Delta G = 0$, was found experimentally to be 2.4 kcal/mol.[1] On the basis of an outer-sphere, adiabatic electron-transfer theory, Marcus[10,11] had previously derived an alternative expression for $\Delta G^{\ddagger}$,

$$\Delta G^{\ddagger} = \Delta G^{\ddagger}_0\ [1 + (\Delta G/4\Delta G^{\ddagger}_0)]^2 \qquad (6)$$

With $\Delta G^{\ddagger}_0$ = 2.4 kcal/mol both eq 5 and 6 together with eq 4 are in good agreement with experimental results for electron-transfer fluorescence quenching of neutral molecules when $\Delta G > -15$ kcal/mol. For more exothermic reactions, however, the Marcus relation (eq 6) predicts a drastic decrease in k_q leading to the "Marcus' inverted region".[1,7,11]

Table IV. Values of $\Delta G^{\ddagger}_0$ for Electron-Transfer Fluorescence Quenching[a]

theory	$Ag^{-}\cdot$	$Ta^{+}\cdot$
Marcus (eq 6)	10.0	15.3
Weller (eq 5)	7.6	9.6

[a] In kcal/mol.

Neither a Weller curve nor a Marcus curve will, however, fit our experimental data when $\Delta G^{\ddagger}_0$ = 2.4 kcal/mol. If we allow $\Delta G^{\ddagger}_0$ to vary, we can obtain a reasonable good fit using the Marcus theory; see Figures 1 and 2. Optimized values of $\Delta G^{\ddagger}_0$ from least-squares fits are listed in Table IV. We cannot test for the presence or absence of the "inverted region" in these systems. This would require very large negative ΔG values (<−50 kcal/mol for $Aq^{-}\cdot$ and <−70 kcal/mol for $Ta^{+}\cdot$). At these highly exothermic reactions the electron transfer would be exothermic even in the ground-state molecules. Apparently the Weller equation is less suited than is the Marcus equation for treatment of the fluorescence data in these systems (see Figures 1 and 2).

As mentioned above, Eberson[7,8] has pointed out that large $\Delta G^{\ddagger}_0$ values may be expected in certain systems. Thus, the electron-transfer reduction of alkyl halides by various donors such as aromatic radical anions and inorganic salts gave $\Delta G^{\ddagger}_0$ = 11.5 kcal/mol.[8b] Here, the large $\Delta G^{\ddagger}_0$ value could be explained by assuming a virtually broken C–halogen bond in the transition state:

$$R\text{-}X + D^{-}\cdot \rightarrow R\cdot + X^{-} + D$$

Similarly, $\Delta G^{\ddagger}_0$ = 10 kcal/mol was found for one-electron reductions of diacyl peroxides.[8a] Using aliphatic amines as electron donors, both Weller[12] and Ballardini et al.[13] have observed variations, although very small ones, from the value 2.4 kcal/mol. We have very recently studied the fluorescence quenching of pyrylium salts.[14] These, however, are best analyzed by using the Weller equation with $\Delta G^{\ddagger}_0$ close to 2.4 kcal/mol.

The main contributions to $\Delta G^{\ddagger}_0$ are solvent reorganization energies due to electron removal from or addition to the involved molecules and bond reorganization energies. The reorganization energy parameter $\lambda_{12} = 4\Delta G^{\ddagger}_0$ connected with the electron transfer from species 1 to 2 may be calculated by the simple equation[7,10]

$$\lambda_{12} = \tfrac{1}{2}(\lambda_1 + \lambda_2) \qquad (7)$$

where λ_1 and λ_2 are reorganization energy parameters associated with the self-exchange reactions, e.g., for 1,

$$A_1^{-}\cdot + A_1 \rightleftharpoons A_1 + A_1^{-}\cdot$$

The parameters λ_1 and λ_2 may be obtained from the broadening of the lines in the EPR spectra if the species involved are long-lived enough for such a measurement. Photochemically excited states are not amenable to such a treatment, and we have therefore attempted to attack the problem by means of theoretical calculations.

The electronic structure of antraquinone has been studied in an attempt to elucidate the results found. The analysis presented here is based mainly on the energy-weighted maximum-overlap (EWMO) model,[15] since accurate calculations are beyond reach for systems of the class considered here. Simons[16] has shown that limited basis set molecular orbital calculations can be unsatisfactory and even misleading. The EWMO model has been used

(10) Marcus, R. A. *J. Phys. Chem.* **1963**, *67*, 853. *Annu. Rev. Phys. Chem.* **1964**, *15*, 155.
(11) Marcus, R. A.; Siders, P. *J. Phys. Chem.* **1982**, *86*, 662. Indelli, M. T.; Scandola, F. *J. Am. Chem. Soc.* **1978**, *100*, 7733. Ratner, M. A.: Levine, R. D. *Ibid.* **1980**, *102*, 4898. Kringler, R. J.; Kochi, J. K. *Ibid.* **1982**, *104*, 4186.
(12) Weller, A., private communications.
(13) Ballardini, R.; Varani, G.; Indelli, M. T.; Scandola, F.; Balzani, V. *J. Am. Chem. Soc.* **1978**, *100*, 7219.
(14) Wintgens, V.; Pouliquen, J.; Simalty, M.; Kossany, J.; Justesen, F. K.; Eriksen, J. *J. Photochem.*, in press.
(15) Linderberg, J.; Öhrn, Y.; "Propagators in Quantum Chemistry"; Academic Press: New York, 1973, Linderberg, J.; Öhrn, Y.; Thulstrup, P. W. *Quantum Sci.* **1976**, 93.
(16) Simons, J. *Annu. Rev. Phys. Chem.* **1977**, *28*, 15.

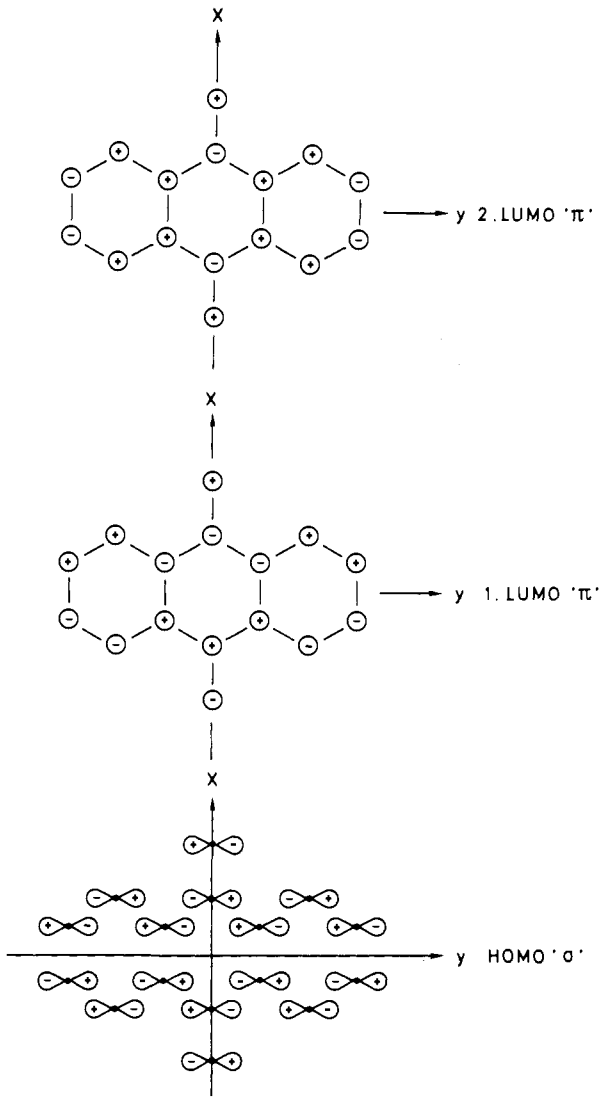

Figure 3. Representation of the forms of the molecular orbital coefficients of the highest occupied and the two lowest unoccupied orbitals in anthraquinone.

to discuss spin resonance features of inorganic radicals with good results[17] and has also recently been found useful in the study of organic radicals.[18]

The fundamental notation in discussing the features of radicals with one unpaired electron spin is the separation of the electron energy

$$E(j,N \pm 1) = E(0,N) \pm e(j) \qquad (8)$$

where $E(0,N)$ represents the closed shell energy of the reference state (in this analysis, the neutral anthraquinone in its ground state) and $e(j)$ is the energy difference between the radical and the ground state. This difference can be obtained from the electron propagator,[15] and the EWMO model was originally presented as an approximate way to estimate the propagator. The result of the approximation is a molecular orbital model where a formally orthogonalized set of atomic orbitals offers a representation of an effective Hamiltonian of the form[17]

$$h_{rr} = -x_r^2$$
$$h_{rs} = -x_r S'_{rs} x_s$$
$$r \neq s \qquad (9)$$

(17) Dalgaard, E. *Proc. R. Soc. London Ser. A* **1978**, *361*, 478. Dalgaard, E.; Linderberg, J. *J. Chem. Phys.* **1976**, *65*, 69. *Int. J. Quantum Chem. Suppl.* **1975**, *9*, 269.
(18) Jones, M. T. de Boer, E. *Mol. Phys.* **1982**, *47*, 487.

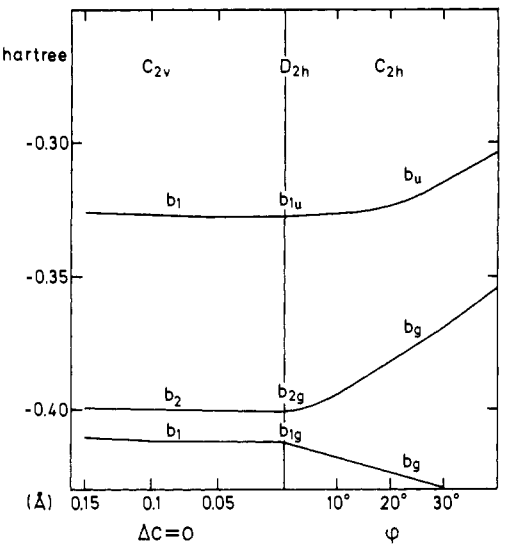

Figure 4. Orbital energies and symmetry classification of $Aq^{-\cdot}$ and their change under two types of distortions of the nuclear conformations from the D_{2h} symmetry. The curves on the left side ($\Delta C = 0$) come from an asymmetric stretch of the two carbonyl bonds, and the curves on the rignt side come from a folding of ring A along 8a–10a and ring C along 4a–9a.

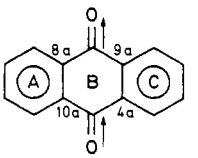

Figure 5. Stretching of the two carbonyl bonds in $Aq^{-\cdot}$*, is shown by the arrows.

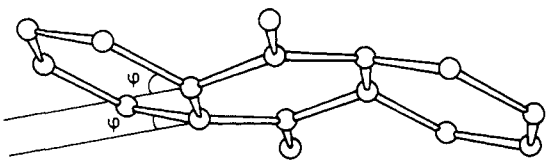

Figure 6. Folding of the side rings (A and C) in $Aq^{-\cdot}$*.

The eigenvalues of this effective Hamiltonian are estimates of the energy difference $e(j)$, and we associate those corresponding to occupied orbitals with $N-1$ electron states and the others with $N+1$ electron states. Lacking a more detailed theory, we attempt to locate other states at energies such as

$$E(jk,l,N+1) = E(0,N) + e(j) + e(k) - e(l) \qquad (10)$$

where the addition of an electron ($e(j)$) is accompanied by an excitation with energy $e(k) - e(l)$. These procedures give poor results when used within the Hartree–Fock (HF) model, since unoccupied orbitals usually have energies in the positive range. The eigenvalues of the effective Hamiltonian (eq 9) are negative and should not be interpreted as approximate molecular orbital energies from an HF calculation.

Conformational changes and other perturbations of the electronic system induce changes in $E(0,N)$ as well as in $e(j)$ and $e(k)$. As the relative position of the states is only determined by the latter, we expect to derive useful information from a study of the possible degeneracies or near degeneracies in the molecular orbitals and eigenvalues of the effective Hamiltonian in the way one usually uses molecular orbital theory.

When mean bond lengths for anthraquinone are used, calculations with the EWMO model result in a spectrum of energy levels where the highest occupied and lowest unoccupied orbitals have the forms shown in Figure 3.

The symmetry classification and orbital energies for the highest occupied molecular orbital and the two lowest unoccupied molecular orbitals are given in Figure 4. The figure also contains the change in these energies under two types of distortions of the

Table V

D_{2h}	E	$C_2(z)$	$C_2(y)$	$C_2(x)$	i	$\sigma(xy)$	$\sigma(xz)$	$\sigma(yx)$
A_g	1	1	1	1	1	1	1	1
B_{1g}	1	1	−1	−1	1	1	−1	−1
B_{2g}	1	−1	1	−1	1	−1	1	−1
B_{3g}	1	−1	−1	1	1	−1	−1	1
A_u	1	1	1	1	−1	−1	−1	−1
B_{1u}	1	1	−1	−1	−1	−1	1	1
B_{2u}	1	−1	1	−1	−1	1	−1	1
B_{3u}	1	−1	−1	1	−1	1	1	−1

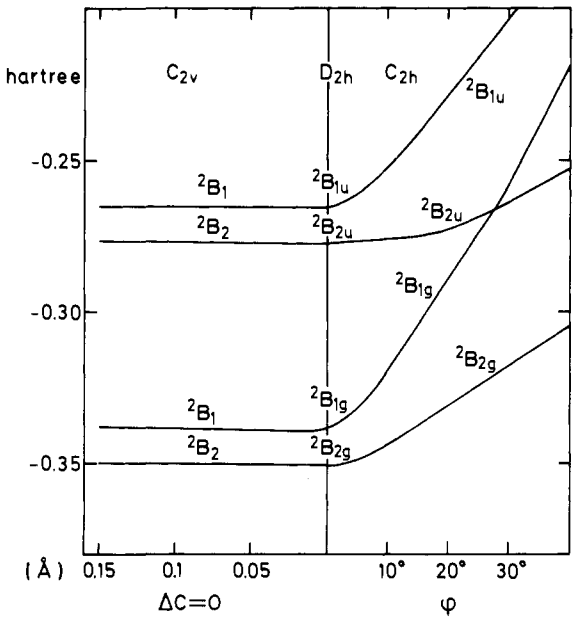

Figure 7. State energies in $Aq^{-}\cdot^{*}$ under the two types of distortions (asymmetric stretch (C_{2v}) and folding of the side rings (C_{2h})).

nuclear conformation from D_{2h} symmetry.

From Figure 4 it appears that an asymmetric stretch of the two carbonyl bonds (Figure 5) causes an almost parallel displacement of the eigenvalues in the lower C_{2v} symmetry.

Another possibility for a distortion in $Aq^{-}\cdot^{*}$ is a folding of ring A along 8a–10a and ring C along 4a–9a, which causes the distortion shown in Figure 6; this results in a splitting of the nearly degenerate b_{1g} and b_{2g} orbitals when going into C_{2h} symmetry.

The symmetry classification derives from Table V.

Since all irreducible representations are one dimensional, it follows that the direct product of B_{1g} and B_{2g} equals B_{3g}, while B_{1u} with B_{3u} gives B_{2g}. Reduction in symmetry through folding rings A and C leads to C_{2h} and the classifications $(A_g, B_{3g}) \rightarrow A_g$, $(B_{1g}, B_{2g}) \rightarrow B_g$, $(A_u, B_{3u}) \rightarrow A_u$, and $(B_{1u}, B_{2u}) \rightarrow B_u$. An asymmetric stretch in the carbonyl bonds causes a reduction to C_{2v} and the classifications $(A_g, B_{3u}) \rightarrow A_1$, $(B_{1g}, B_{2u}) \rightarrow B_1$ $(B_{2g}, B_{1u}) \rightarrow B_2$, and $(B_{2g}, A_u) \rightarrow A_2$. These rules allow us to characterize the low-lying states.

State energies are given in Figure 7, and the effect of distortions is shown as in Figure 4. By comparison of the states in Figure 7 it is seen that the distinctive feature is the lowering of the $^2B_{1u}$ state relative to the $^2B_{1g}$ and $^2B_{2g}$ states. It is found in the EWMO model that the ground state of the anion should be classified as a $^2B_{2g}$ state, a result in agreement with almost any molecular orbital theory. The present analysis places a $^2B_{1g}$ state, which is of the same symmetry as an $n\pi^*$ excited state, rather close in energy (~0.01 au). Similarly, a $^2B_{2u}$ state is rather close to the $^2B_{1u}$ state.

From the present analysis we predict the anion ground state of anthraquinone to have essentially the same geometry as the neutral molecule. The nearby $^2B_{1g}$ state is located only 0.4 eV above the ground state. Its existence should be difficult to ascertain since there are no allowed optical transitions to the other state. The magnetic circular dichroism of the absorption from the ground state to the $^2B_{1u}$ state might give an indication of the presence of a low-lying state of $^2B_{1g}$ symmetry.

The photoexcited state of $Aq^{-}\cdot$ is placed 1.9 eV (expt 2.21 eV[6]) above the ground state, and the transition moment vector is parallel with the carbonyl bonds, since the direct product of B_{2g} and B_{1u} is B_{3u}. It appears that this state has a saddle point on the electronic energy hypersurface at the symmetric geometry and that a relaxation through a displacement along a b_{3g} symmetry coordinate will reduce the electronic energy relative to the ground state. The most effective distortion direction of $Aq^{-}\cdot^{*}$ can be determined from gradients of the matrix (eq 9), and our calculations show that a simple folding (Figure 6) of rings A and C gives the most rapid decrease in energy.

This calculated geometry difference between $Aq^{-}\cdot$ and $Aq^{-}\cdot^{*}$ is supported by the relatively large Stoke shift (ca. 1200 cm^{-1}) obtained from the fluorescence emission and excitation spectrum of $Aq^{-}\cdot$.

The asymmetric stretching of the carbonyl bonds (Figure 5) is not effective in changing the electronic energy in the present model whereas this mechanism seems to be dominant in other anions.[19] A minimal basis set (STO-3G) calculation with GAUSSIAN 80[20] gives a different ordering of the occupied orbitals and does indicate that the carbon–oxygen distance is operative in changing the energy, but geometry optimization could not be carried through and was not judged to be warranted in view of the inherent uncertainties in calculation of this type for negative ions.[16] Calculation within an INDO program gives a spectrum of nearly the same kind as EWMO.

A comparison of the atomic net charges in Aq and $Aq^{-}\cdot^{*}$ shows that the extra electron in $Aq^{-}\cdot$ and $Aq^{-}\cdot^{*}$ is located in the rings and that only a very low charge transfer takes place from the center ring to the side rings in $Aq^{-}\cdot^{*}$. A contribution to $\Delta G^{\ddagger}_0$ from a sudden polarization in $Aq^{-}\cdot^{*}$ followed by a reorganization in the solvent seems to play a minor role compared with the changes through the bending of the rings.

In conclusion, we have shown that the Marcus theory is well suited for analyzing electron-transfer fluorescene quenching of radical ions. The reaction is accompanied by large reorganization energies which on the basis of EWMO calculations may be understood as large geometric changes in the transition state of the electron-transfer step.

Acknowledgment. Thanks are expressed to The Danish Natural Science Research Council for a predoctoral fellowship to one of us (K.A.J.).

Registry No. $Ag^{-}\cdot$, 3426-73-1; $Ta^{+}\cdot$, 34507-27-2.

(19) Linderberg, J.; Ratner, M. A. *J. Am. Chem. Soc.* **1981**, *103*, 3265.
(20) Binkley, J. S., Whiteside, R. A.; Krishnan, R.; Seeger, R.; DeFrees, D. J.; Schlegel, H. B.; Topiol, S.; Kalm, L. R.; Pople, J. A. *QCPE* **1980**, *13*, 406.